

Day-Night Effect in Solar Neutrino Oscillations with Three Flavors

Mattias Blennow^{a*}, Tommy Ohlsson^{a†}, Håkan Snellman^{a‡}

^a*Division of Mathematical Physics, Department of Physics, Royal Institute of Technology (KTH) - AlbaNova University Center, Roslagstullsbacken 11, 106 91 Stockholm, Sweden*

Abstract

We investigate the effects of a non-zero leptonic mixing angle θ_{13} on the solar neutrino day-night asymmetry. Using a constant matter density profile for the Earth and well-motivated approximations, we derive analytical expressions for the ν_e survival probabilities for solar neutrinos arriving directly at the detector and for solar neutrinos which have passed through the Earth. Furthermore, we numerically study the effects of a non-zero θ_{13} on the day-night asymmetry at detectors and find that they are small. Finally, we show that if the uncertainties in the parameters θ_{12} and Δm^2 as well as the uncertainty in the day-night asymmetry itself were smaller than they are today, this effect could, in principle, be used to determine θ_{13} .

PACS: 14.60.Pq, 13.15.+g, 26.65.+t

Key words: neutrino oscillations, matter effects, solar neutrinos, solar neutrino day-night effect

1. Introduction

Neutrino oscillation physics has entered the era of precision measurements with the results from the Super-Kamiokande [1], SNO [2, 3, 4, 5], and KamLAND [6] experiments. Especially, there has recently come impressive results from measurements of solar neutrinos (see Refs. [4, 5, 7]) and the solar neutrino problem has successfully been solved in terms of solar neutrino oscillations.

The solar neutrino day-night effect, which measures the relative difference of the electron neutrinos coming from the Sun at night- and daytime, is so far the best long baseline experiment that can measure the matter effects on the neutrinos, the so-called Mikheyev-Smirnov-Wolfenstein (MSW) effect [8]. In all accelerator long baseline experiments, the neutrinos cannot be made to travel through vacuum. The atmospheric neutrino experiments, on the other hand, use different baseline lengths for neutrinos traversing the Earth and those that pass through vacuum. With the advent of the precision era in neutrino oscillation

physics, we can gradually hope to obtain better measurements of the day-night effect. Recently, both Super-Kamiokande and SNO have presented new measurements [4, 7] of this effect that have errors approaching a few standard deviations in significance.

In this paper, we analyze the day-night effect in the three neutrino flavor case. Earlier analyzes of this effect have with a few exceptions been performed for the two neutrino flavor case. Furthermore, the present data also permit a new treatment of the effect, due to the particular values of leptonic mixing angles and neutrino mass squared differences obtained from other experiments. There are six parameters that describe the neutrinos in the minimal extension of the standard model: three leptonic mixing angles θ_{12} , θ_{13} , and θ_{23} , one CP-phase δ , and two neutrino mass squared differences $\Delta M^2 = m_3^2 - m_1^2$ and $\Delta m^2 = m_2^2 - m_1^2$. At present, there is no evidence for CP violation in neutrino physics, and thus, we will put $\delta = 0$. The solar neutrino day-night effect is mainly sensitive to the angles θ_{12} and θ_{13} , and the mass squared difference Δm^2 . Our goal is to obtain a relatively simple analytic expression for the day-night asymmetry that re-

*E-mail: mbl@theophys.kth.se

†E-mail: tommy@theophys.kth.se

‡E-mail: snell@theophys.kth.se

produces the main features of the situation. It turns out that one can come a long way towards this goal.

Earlier treatments of the day-night effect can be found in Refs. [9, 10, 11, 12, 13]. Our three flavor treatment is consistent with the modifications presented by de Holanda and Smirnov [12] as well as Bandyopadhyay *et al.* [13].

This paper is organized as follows. In Sec. 2, we investigate the electron neutrino survival probability with n flavors for solar neutrinos arriving at the Earth and for solar neutrinos going through the Earth. Next, in Sec. 3, we study the case of three neutrino flavors including production and propagation in the Sun as well as propagation in the Earth. At the end of this section, we present the analytical expression for the day-night asymmetry. Then, in Sec. 4, we discuss the day-night effect at detectors. Especially, we calculate the elastic scattering day-night asymmetry at the Super-Kamiokande experiment and the charged-current day-night asymmetry at the SNO experiment. Furthermore, we discuss the possibility of determining the leptonic mixing angle θ_{13} using the day-night asymmetry. In Sec. 5, we present our summary as well as our conclusions. Finally, in the Appendix, we shortly review for completeness the day-night asymmetry in the case of two neutrino flavors.

2. The n flavor solar neutrino survival probability

Assuming an incoherent neutrino flux [10, 11], the ν_e survival probability for solar neutrinos is

$$P_S = \sum_{i=1}^n k_i |\langle \nu_e | \nu_i \rangle|^2 = \sum_{i=1}^n k_i |U_{ei}|^2, \quad (1)$$

where n is the number of neutrino flavors and k_i is the fraction of the mass eigenstate $|\nu_i\rangle$ in the flux of solar neutrinos. From unitarity it follows that

$$\sum_{i=1}^n k_i = 1. \quad (2)$$

In the case of even mixing, i.e., $k_i = 1/n$ for all i , we obtain $P_S = 1/n$.

For neutrinos reaching the Earth during daytime (at the detector site), P_S is the ν_e survival probability at the detector. However, during nighttime this survival probability may be altered by the influence of the effective Earth matter density potential. Thus, in this case, the survival probability becomes

$$P_{SE} = \sum_{i=1}^n k_i |\langle \nu_e | \tilde{\nu}_i \rangle|^2, \quad (3)$$

where $|\tilde{\nu}_i\rangle = |\nu_i(L)\rangle$ and L is the length of the neutrino path through the Earth. Here, the components of $|\nu_i(t)\rangle$ satisfy the Schrödinger equation

$$i \frac{d|\nu_i(t)\rangle_m}{dt} = H_m |\nu_i(t)\rangle_m \quad (4)$$

with the initial condition $|\nu_i(0)\rangle = |\nu_i\rangle$ and where m denotes the mass eigenstate basis.

The Hamiltonian H is given by

$$H_m \simeq \frac{M^2}{2p} + U^\dagger \text{diag}(V_{CC}, 0, \dots, 0) U, \quad (5)$$

where $M = \text{diag}(m_1, m_2, \dots, m_n)$ and the effective Earth matter density potential is $V_{CC} = \sqrt{2}G_F N_e$, where G_F is the Fermi coupling constant and N_e the electron number density, is a function of t depending on the Earth matter density profile, which is normally given by the Preliminary Reference Earth Model (PREM) [14]. The term $|\langle \nu_e | \tilde{\nu}_i \rangle|^2$ is interpreted as the probability of a neutrino reaching the Earth in the mass eigenstate $|\nu_i\rangle$ to be detected as an electron neutrino after traversing the distance L in the Earth. For notational convenience we denote

$$P_{ie} = |\langle \nu_e | \tilde{\nu}_i \rangle|^2. \quad (6)$$

Clearly, $P_{ie}(L = 0) = |\langle \nu_e | \nu_i \rangle|^2 = |U_{ei}|^2$. Furthermore, from unitarity it follows that

$$\sum_{i=1}^n P_{ie} = 1. \quad (7)$$

Again, in the case of even mixing, we obtain $P_{SE} = 1/n$, and the ν_e survival probability is unaffected by the passage through the Earth.

3. The case of three neutrino flavors

Until now most analyzes of the day-night effect have been done in the framework of two neutrino flavors. However, we know that there are (at least) three neutrino flavors. The reason for using two flavor analyzes has been that the leptonic mixing angle θ_{13} is known to be small [15], leading to an approximate two neutrino case. One of the main goals of this paper is to find the effects on the day-night asymmetry induced by using a non-zero mixing angle θ_{13} .

We will use the standard parameterization of the 3×3 leptonic mixing matrix [16] ($\delta = 0$)

$$U = \begin{pmatrix} c_{13}c_{12} & c_{13}s_{12} & s_{13} \\ * & * & * \\ * & * & * \end{pmatrix}, \quad (8)$$

where $s_{ij} = \sin \theta_{ij}$ and $c_{ij} = \cos \theta_{ij}$, θ_{ij} are leptonic mixing angles, and the elements denoted by * do not affect the neutrino oscillation probabilities, which we are calculating in this paper.

3.1. Production and propagation in the Sun

In the three flavor framework, there are a number of issues of the neutrino production and propagation in the Sun, which are not present in the two flavor framework. First of all, the three energy levels of neutrino matter eigenstates in general allow two MSW resonances. Furthermore, the matter dependence of the mixing parameters are far from as simple as in the two flavor case. The result of this is that we have to make certain approximations.

Repeating the approach made in the two flavor case (see App. A), we obtain the following expression for k_i

$$k_i = \int_0^{R_\odot} dr f(r) \sum_{j=1}^3 |\hat{U}_{ej}|^2 P_{ji}^s, \quad (9)$$

where \hat{U} is the mixing matrix in matter, P_{ji}^s the probability of a neutrino created in the matter eigenstate $|\nu_{M,j}\rangle$ to exit the Sun in the mass eigenstate $|\nu_i\rangle$, and $f(r)$ is the normalized spatial production distribution in the Sun.

The second resonance in the three flavor case occurs at $V_{CC} \simeq \cos(2\theta_{13})\Delta M^2/(2E)$, assuming

that the resonances are fairly separated. The maximal electron number density in the Sun, according to the Standard Solar Model (SSM) [17], is about $N_{e,\max} \simeq 102 N_A/\text{cm}^3$, yielding a maximal effective potential $V_{CC,\max} \simeq 7.8 \cdot 10^{-18}$ MeV. Assuming the large mass squared difference ΔM^2 to be of the order of the atmospheric mass squared difference ($|\Delta m_{\text{atm}}^2| \simeq 2 \cdot 10^{-3}$ eV² [18]), the neutrino energy E to be of the order of 10 MeV, and θ_{13} to be small, we find $\left| \frac{\Delta M^2}{2E} \right| \cos(2\theta_{13}) \simeq 10^{-16}$ MeV. Thus, the solar neutrinos never pass through the second resonance, independent of the sign of the large mass squared difference.

Since the neutrinos never pass through the second resonance, it is a good approximation to assume that the matter eigenstate $|\nu_{M,3}\rangle$ evolves adiabatically, and thus, we have

$$P_{3k}^s = P_{k3}^s = \delta_{3k}. \quad (10)$$

Unitarity implies that

$$P_{12}^s = P_{21}^s = P_{\text{jump}}. \quad (11)$$

Furthermore, if we assume that $V_{CC} \lesssim \Delta m^2/(2E) \ll \Delta M^2/(2E)$, the neutrino evolution is well approximated by the energy eigenstate $|\nu_{M,3}\rangle$ evolving as the mass eigenstate $|\nu_3\rangle$ and the remaining neutrino states oscillating according to the two flavor case with the effective potential $V_{\text{eff}} = c_{13}^2 V_{CC}$. This does not change the probability P_{jump} as calculated with a linear approximation of the potential in the two flavor case. This means that we may use the same expression as that obtained in the two flavor case, see App. A, even if the resonance point, where $|N_e/\bar{N}_e|$ is to be evaluated, does change. However, in the Sun, N_e is approximately exponentially decaying with the radius of the Sun, leading to $|N_e/\bar{N}_e|$ being approximately constant, and thus, independent of the point of evaluation. For the large mixing angle (LMA) region, the probability P_{jump} of a transition from $|\nu_{M,1}\rangle$ to $|\nu_{M,2}\rangle$, or vice versa, is negligibly small ($P_{\text{jump}} < 10^{-1700}$). However, we keep it in our formulas for completeness.

To make one further approximation, as long as the Sun's effective potential is much less than the

large mass squared difference ΔM^2 , the mixing angle $\hat{\theta}_{13} \simeq \theta_{13}$ giving

$$k_3 \simeq \int_0^{R_\odot} dr f(r) \sin^2 \theta_{13} = \sin^2 \theta_{13}. \quad (12)$$

A general parameterization for k_1 and k_2 is then given by

$$k_1 = c_{13}^2 \frac{1 + D_{3\nu}}{2}, \quad k_2 = c_{13}^2 \frac{1 - D_{3\nu}}{2}. \quad (13)$$

In the above approximation, the oscillations between the matter eigenstates $|\nu_{M,1}\rangle$ and $|\nu_{M,2}\rangle$ are well approximated by a two flavor oscillation, using the small mass difference squared Δm^2 , the mixing angle θ_{12} , and the effective potential $V_{\text{eff}} = c_{13}^2 V_{CC}$. Thus, we obtain

$$D_{3\nu} = \int_0^{R_\odot} dr f(r) \cos(2\hat{\theta}_{12}(r))(1 - 2P_{\text{jump}}), \quad (14)$$

where $\cos(2\hat{\theta}_{12}(r))$ is calculated in the same way as in the two flavor case using the effective potential. For reasonable values of the neutrino oscillation parameters, this turns out to be an excellent approximation.

Inserting the above approximation into Eq. (1) with $n = 3$, we obtain

$$P_S = s_{13}^4 + c_{13}^4 \frac{1 + D_{3\nu} \cos(2\theta_{12})}{2}. \quad (15)$$

When $\theta_{13} \rightarrow 0$, we have $D_{3\nu} \rightarrow D_{2\nu}$, and thus, we recover the two flavor survival probability in this limit.

3.2. Propagation in the Earth

As in the case of propagation in the Sun, $V_{CC} \lesssim \Delta m^2/2E \ll \Delta M^2/2E$, $|\nu_{M,3}\rangle \simeq |\nu_3\rangle$, and the remaining two neutrino eigenstates evolve according to the two flavor case with an effective potential of $V_{\text{eff}} = c_{13}^2 V_{CC}$. For the MSW solutions of the solar neutrino problem along with the assumption that ΔM^2 is of the same order of magnitude as the atmospheric mass squared difference, this condition is well fulfilled for solar neutrinos propagating through the Earth. As a direct result, we obtain the probability P_{3e} as

$$P_{3e} \simeq |\langle \nu_e | \nu_3 \rangle|^2 = |U_{e3}|^2 = s_{13}^2. \quad (16)$$

It also follows that

$$P_{2e} = c_{13}^4 \frac{KV_E}{4a^2} \sin^2(2\theta_{12}) \sin^2(aL) + c_{13}^2 s_{12}^2, \quad (17)$$

where

$$a = \frac{1}{2} \sqrt{K^2 - 2c_{13}^2 V_E K \cos(2\theta_{12}) + c_{13}^4 V_E^2}, \quad (18)$$

V_E is the effective electron neutrino potential in the Earth, and $K = \frac{\Delta m^2}{2E}$. We observe that when $L = 0$ or $V_E = 0$, $P_{2e} = c_{13}^2 s_{12}^2 = |U_{e2}|^2$ just as expected.

3.3. The final expression for P_{n-d}

Now, we insert the analytical expressions obtained in the previous two sections into Eq. (3) with $n = 3$ and subtract P_S from this in order to obtain an expression for $P_{n-d} = P_{SE} - P_S$ in the three flavor framework. After some simplifications, we find

$$P_{n-d} = -c_{13}^6 D_{3\nu} \frac{KV_E}{4a^2} \sin^2(2\theta_{12}) \sin^2(aL). \quad (19)$$

For the MSW solutions of the solar neutrino problem, $K \gg c_{13}^2 V_E$, and thus, $a \simeq \frac{K}{2}$. This yields

$$P_{n-d} \simeq -2c_{13}^6 D_{3\nu} \frac{EV_E}{\Delta m^2} \sin^2(2\theta_{12}) \sin^2\left(\frac{\Delta m^2}{4E} L\right). \quad (20)$$

Apparently, the effect of using three flavors instead of two is, up to the approximations made, a multiplication by c_{13}^6 as well as a correction in changing $D_{2\nu}$ to $D_{3\nu}$. When $\theta_{13} \rightarrow 0$, we have $D_{3\nu} \rightarrow D_{2\nu}$, and we regain the two flavor expression in this limit (see App. A). An important observation is that the regenerative term, for $V_E \ll K$, is linearly dependent on V_E . Thus, the choice of which value of V_E to use is crucial for the quantitative result. As is argued in the appendix, the potential to use is the potential corresponding to the electron number density of the Earth's crust. However, the qualitative behavior of the effect of a non-zero θ_{13} is not greatly affected.

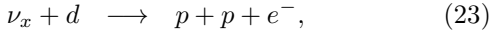
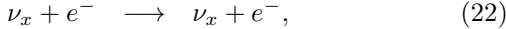
4. The day-night effect at detectors

From the calculations made in the previous parts of this paper, we obtain the day-night asymmetry of the electron neutrino flux at the neutrino

energy E as

$$\begin{aligned} A_{n-d}^{\phi_e}(E) &= 2 \frac{\phi_{e,N}(E) - \phi_{e,D}(E)}{\phi_{e,N}(E) + \phi_{e,D}(E)} \\ &= \frac{P_{n-d}(E)}{P_S(E) + \frac{P_{n-d}(E)}{2}}. \end{aligned} \quad (21)$$

However, this is *not* the event rate asymmetry measured at detectors. We will assume a water-Cherenkov detector in which neutrinos are detected by one of the following reactions⁴



where $x = e, \mu, \tau$, which are referred to as elastic scattering (ES) and charged-current (CC), respectively. The CC reaction can only occur for $x = e$, since inserting $x \neq e$ in Eq. (23) would violate the lepton numbers L_e and L_x . We assume that the scattered electron energy T' is measured and that the cross-sections $d\sigma_{\nu_\mu}/dT'$ and $d\sigma_{\nu_\tau}/dT'$ are equal.

If we denote the zenith angle, i.e., the angle between zenith and the Sun at the detector, by α , then the event rate of measured electrons with energy T in the detector is proportional to

$$\begin{aligned} R(\alpha, T) &= \int_0^\infty dE \phi(E) \int_0^{T'_{\max}} dT' \\ &\times F(T, T') \frac{d\sigma_{\nu_{\text{solar}}}}{dT'}, \end{aligned} \quad (24)$$

where $\phi(E)$ is the total solar neutrino flux, T' is the true electron energy, and $d\sigma_{\nu_{\text{solar}}}/dT'$ is given by

$$\frac{d\sigma_{\nu_{\text{solar}}}}{dT'} = P_{SE} \frac{d\sigma_{\nu_e}}{dT'} + (1 - P_{SE}) \frac{d\sigma_{\nu_\mu}}{dT'}. \quad (25)$$

Here, we have used the assumption $d\sigma_{\nu_\mu}/dT' = d\sigma_{\nu_\tau}/dT'$, since neutrinos not found in the state $|\nu_e\rangle$ are assumed to be in the state $|\nu_\mu\rangle$ or in the state $|\nu_\tau\rangle$. The energy resolution of the detector is introduced through $F(T, T')$, which is given by

$$F(T, T') = \frac{1}{\Delta_{T'} \sqrt{2\pi}} \exp \left(-\frac{(T - T')^2}{2\Delta_{T'}^2} \right), \quad (26)$$

⁴For the neutral-current (NC) reaction, $\nu_x + d \rightarrow p + n + \nu_x$, the cross sections for all neutrino flavors are the same to leading order in the weak coupling constant. As a result, there will be no day-night effect in the NC reaction.

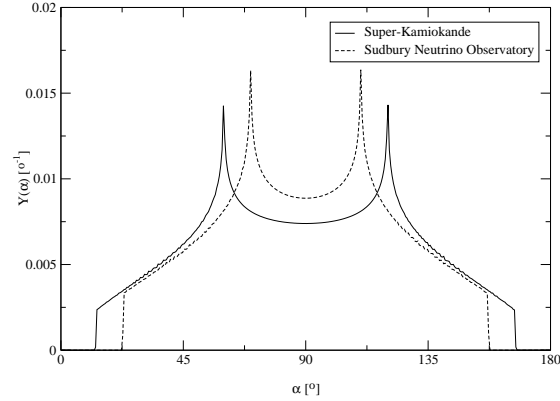


Figure 1. The zenith angle exposure function $Y(\alpha)$ for SK and SNO as a function of the zenith angle α . The data are retrieved from Ref. [19].

where $\Delta_{T'}$ is the energy resolution at the electron energy T' .

The night and day rates N and D at the measured electron energy T are given by

$$D(T) = \int_0^{\frac{\pi}{2}} d\alpha R(\alpha, T) Y(\alpha), \quad (27)$$

$$N(T) = \int_{\frac{\pi}{2}}^{\pi} d\alpha R(\alpha, T) Y(\alpha), \quad (28)$$

respectively. Here, $Y(\alpha)$ is the zenith angle exposure function, which gives the distribution of exposure time for the different zenith angles. The exposure function is clearly symmetric around $\alpha = \frac{\pi}{2}$ and is plotted in Fig. 1 for both Super-Kamiokande (SK) and SNO. From the night and day rates at a specific electron energy, we define the day-night asymmetry at energy T as

$$A_{n-d}(T) = 2 \frac{N(T) - D(T)}{N(T) + D(T)}. \quad (29)$$

The final day-night asymmetry is given by integrating the day and night rates over all energies above the detector threshold energy T_{th} , i.e.,

$$A_{n-d} = 2 \frac{\int_{T_{\text{th}}}^{\infty} dT (N(T) - D(T))}{\int_{T_{\text{th}}}^{\infty} dT (N(T) + D(T))} = 2 \frac{N - D}{N + D}.$$

(30)

The threshold energy T_{th} is 5 MeV for both SK and SNO.

For computational reasons, we will start by performing the integral over the zenith angle α . For the daytime flux D , $P_{SE} = P_S$, which is independent of α . As a result, the only α dependence is in $Y(\alpha)$ and the zenith angle integral only contributes with a factor one-half (if the normalization of Y is such that $\int_0^\pi d\alpha Y(\alpha) = 1$). In order to be able to use the results we have obtained for P_{n-d} , we need to compute the difference between the night and day fluxes, which is given by

$$N(T) - D(T) = \int_{\frac{\pi}{2}}^{\pi} d\alpha Y(\alpha) R^{n-d}, \quad (31)$$

where the quantity $R^{n-d} = R(\alpha, T) - R(\pi - \alpha, T)$ is on the form

$$\begin{aligned} R^{n-d} = & \int_0^\infty dE_\nu \phi(E_\nu) \int_0^{T'_{\text{max}}} dT' \\ & \times F(T, T') \frac{d\sigma_{\nu_{\text{sol}}}^{n-d}}{dT'} \end{aligned} \quad (32)$$

and

$$\frac{d\sigma_{\nu_{\text{sol}}}^{n-d}}{dT'} = P_{n-d}(\alpha, E_\nu) \left(\frac{d\sigma_{\nu_e}}{dT'} - \frac{d\sigma_{\nu_\mu}}{dT'} \right). \quad (33)$$

Note that the α dependence in P_{n-d} enters through the length traveled by the neutrinos in the Earth and that the argument aL of the second \sin^2 -factor in Eq. (19) oscillates very fast and performs an effective averaging of P_{n-d} in the zenith angle integral, i.e., replacing $\sin^2(aL)$ by 1/2. After this averaging, the only zenith angle dependence left is that of $Y(\alpha)$ and the zenith angle integral only gives us a factor of one-half as in the case of the day rate D .

4.1. Elastic scattering detection

Neutrinos are detected through ES at both SK and SNO. The ES cross-sections in the laboratory frame are given by Ref. [16]. For kinematical reasons, the maximal kinetic energy of the scattered electron in the laboratory frame is given by

$$T'_{\text{max}} = \frac{E_\nu}{1 + \frac{m_e}{2E_\nu}}. \quad (34)$$

The integrals that remain cannot be calculated analytically. Hence, we use numerical methods to evaluate these integrals. However, computing all integrals by numerical methods demand a lot of computer time, and thus, we make one further approximation, that all solar ${}^8\text{B}$ neutrinos are produced where the solar effective potential is $V_{CC} \simeq 7.07 \cdot 10^{-18}$ MeV, which is the effective potential at the radius where most solar neutrinos are produced. For reasonable values of the fundamental neutrino parameters, the error made in this approximation is small.

For the energy resolution of SK, we use [10]

$$\Delta_{T'} = 1.6 \text{ MeV} \sqrt{T'/(10 \text{ MeV})}, \quad (35)$$

and for the electron number density in the Earth, we use $N_e = 1.4 N_A / \text{cm}^3$, where N_A is the Avogadro constant, which roughly corresponds to 2.8 g/cm³ (using $Z/A \simeq 0.5$, where Z is the number of protons and A the number of nucleons for the mantle of the Earth). The electron number density used corresponds to the density in the Earth's crust. The motivation for using this density rather than a mean density can be found in App. A. Note that the regenerative term P_{n-d} in Eq. (20), and thus, the day-night asymmetry, is linearly dependent on the matter potential V_E . It follows that the electron number density used has a great impact on the final results. If we had used the average mantle matter density of about 5 g/cm³, then the resulting asymmetry would increase by almost a factor of two.

The above values give us the numerical results presented in Fig. 2. As can be seen from this figure, the relative effect of a non-zero θ_{13} is increasing if the small mass squared difference Δm^2 increases or if the measured electron energy or the leptonic mixing angle θ_{12} decreases. The effect of changing θ_{12} is also clearly larger for smaller electron energy T and larger small mass squared difference Δm^2 . In Fig. 3, the isocontours of constant day-night asymmetry in the SK detector with θ_{13} equal to 0 and 9.2° are shown for a parameter space covering the LMA solution of the solar neutrino problem. As can be seen from this figure, the variation in the isocontours are small compared to the size of the LMA solution and

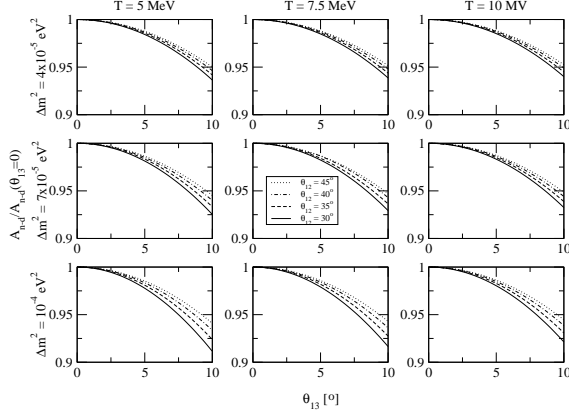


Figure 2. The day-night asymmetry at SK for different values of T , Δm^2 , and θ_{12} as a function of θ_{13} relative to the corresponding value for $\theta_{13} = 0$.

to the current uncertainty in the day-night asymmetry [4, 7]. However, if the values of the parameters θ_{12} , Δm^2 , and A_{n-d} were known with a larger accuracy, then the change due to non-zero θ_{13} could, in principle, be used to determine the “reactor” mixing angle θ_{13} as an alternative to long baseline experiments such as neutrino factories [20, 21] and super-beams [20, 22, 23] as well as future reactor experiments [22] and matter effects for supernova neutrinos [24]. The day-night asymmetry for the best-fit value of Ref. [18] is $A_{n-d} \simeq 3.0\%$, which is larger than the theoretical value quoted by the SK experiment [7], but still clearly within one standard deviation of the experimental best-fit value.

4.2. Charged-current detection

Only SNO uses heavy water, and thus, SNO is the only experimental facility detecting solar neutrinos through the CC reaction (23). Since the electron mass m_e is much smaller than the proton mass m_p ($m_e \simeq 511$ keV, $m_p \simeq 938$ MeV), most of the kinetic energy in the center-of-mass frame, which is well approximated by the laboratory frame, since the deuteron mass by far exceeds

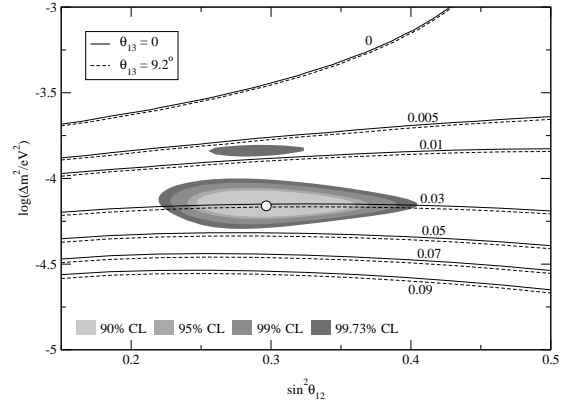


Figure 3. Isocontours in the θ_{12} - Δm^2 parameter space for the ES day-night asymmetry for two different values of θ_{13} . The values of A_{n-d} for the different isocontours are shown in the figure. The shaded regions correspond to the allowed regions of the parameter space for different confidence levels and the circle corresponds to the best-fit point according to Ref. [18].

the neutrino momentum, after the CC reaction will be carried away by the electron. This energy is given by

$$T' = E + \Delta E_{\text{mass}}, \quad (36)$$

where $\Delta E_{\text{mass}} = m_d - 2m_p - m_e \simeq -1.95$ MeV. Thus, we approximate the differential cross-section $d\sigma_{\nu_e}/dT'$ by

$$\frac{d\sigma_{\nu_e}}{dT'} = \sigma_{\nu_e} \delta(T' - E + 1.95 \text{ MeV}). \quad (37)$$

In the above expression, we use the numerical results given in Ref. [25] and perform linear interpolation to calculate the total cross-section σ_{ν_e} as a function of the neutrino energy E . For $x \neq e$, the reaction in Eq. (23) is forbidden, since it violates the lepton numbers L_e and L_x . Thus, for $x \neq e$, we have $d\sigma_{\nu_x}/dT' = 0$.

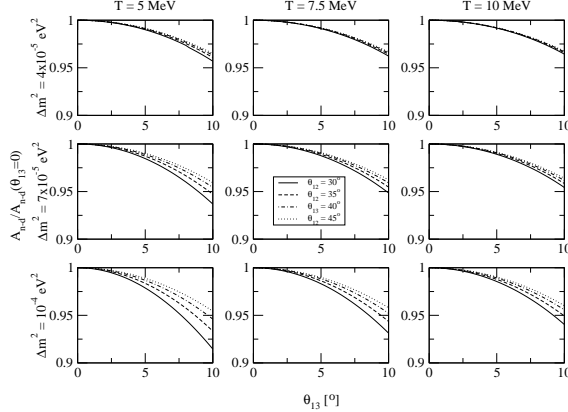


Figure 4. The CC day-night asymmetry at SNO for different values of T , Δm^2 , and θ_{12} as a function of θ_{13} relative to the corresponding value for $\theta_{13} = 0$.

The energy resolution at SNO is given by [3,26]

$$\begin{aligned} \Delta_{T'} &= -0.0684 \text{ MeV} \\ &+ 0.331 \text{ MeV} \sqrt{(T'/\text{MeV})} \\ &+ 0.0425 \text{ MeV} (T'/\text{MeV}). \end{aligned} \quad (38)$$

This gives the results presented in Fig. 4. This figure shows the same main features as Fig. 2. However, the effects of different T and Δm^2 are larger in the CC case.

In Fig 5, we have plotted isocontours for the CC day-night asymmetry for θ_{13} equal to 0 and 9.2° in order to observe the effect of a non-zero θ_{13} for the day-night asymmetry isocontours in the region of the LMA solution. Just as in the case of ES, the isocontours do not change dramatically and the change is small compared to the uncertainty in the day-night asymmetry. It is also apparent that the day-night asymmetry is smaller for the ES detection than for the CC detection. This is to be expected, since the ES detection is sensitive to the fluxes of ν_μ and ν_τ as well as to the ν_e flux, while the CC detection is only sensitive to the ν_e flux. The day-night asymmetry for the best-fit values of Ref. [18] is

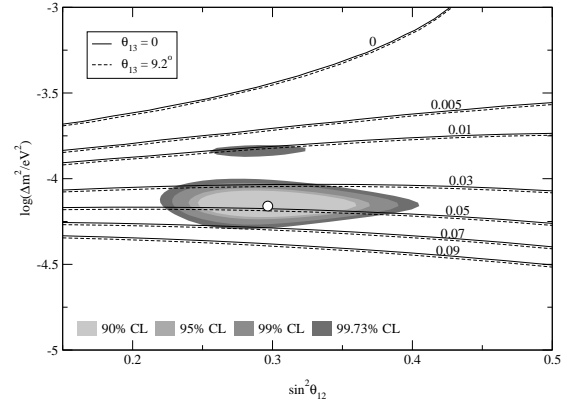


Figure 5. Isocontours for the CC day-night asymmetry in the θ_{12} - Δm^2 parameter space for two different values of θ_{13} . The values of A_{n-d} for the different isocontours are shown in the figure. The shaded regions and the circle are the same as in Fig. 3.

$A_{n-d} \simeq 4.7\%$, which corresponds rather well to the values presented in Refs. [12, 13].

4.3. Determination of θ_{13} using the day-night asymmetry

As we observed earlier, the day-night asymmetry can, in principle, be used for determining the mixing angle θ_{13} if the experimental uncertainties in Δm^2 , θ_{12} , and the day-night asymmetry itself were known to a larger accuracy. We now ask how small the above uncertainties must be to obtain a reasonably low uncertainty in θ_{13} . To estimate the uncertainty $\delta\theta_{13}$ in θ_{13} , we use the pessimistic expression

$$\begin{aligned} \delta\theta_{13} &\simeq \left| \frac{\partial\theta_{13}}{\partial A_{n-d}} \right| \delta A_{n-d} + \left| \frac{\partial\theta_{13}}{\partial\theta_{12}} \right| \delta\theta_{12} \\ &+ \left| \frac{\partial\theta_{13}}{\partial\Delta m^2} \right| \delta\Delta m^2. \end{aligned} \quad (39)$$

Let us suppose that, some time in the future, we have determined the best-fit values for the parameters Δm^2 and θ_{12} to be $\Delta m^2 = 6.9 \cdot 10^{-5} \text{ eV}^2$ and $\theta_{12} = 33.2^\circ$ with the uncertainties $\delta\Delta m^2 \simeq 2.5 \cdot 10^{-6} \text{ eV}^2$ and $\delta\theta_{12} \simeq$

0.5° . Furthermore, suppose that we have measured the day-night asymmetry for the ES reaction to be $A_{n-d} \simeq 0.03$ with an uncertainty $\delta A_{n-d} \simeq 0.002$. These uncertainties roughly correspond to one tenth of the uncertainties of today's measurements. Next, we estimate the partial derivatives of Eq. (39) numerically and obtain $\partial\theta_{13}/\partial A_{n-d} \simeq -3000^\circ$, $\partial\theta_{13}/\partial\theta_{12} \simeq 0.4$, and $\partial\theta_{13}/\partial\Delta m^2 \simeq -2 \cdot 10^{6^\circ}/\text{eV}^2$. This gives an estimated error in θ_{13} of $\delta\theta_{13} \simeq 12^\circ$ with 6.6° from the uncertainty in A_{n-d} , 5.2° from the uncertainty in Δm^2 and 0.2° from the uncertainty in θ_{12} . (Using the uncertainties $\delta\Delta m^2 \simeq 0.8 \cdot 10^{-6}$ eV 2 and $\delta\theta_{12} \simeq 4^\circ$ suggested in Ref. [27], we obtain the uncertainty $\delta\theta_{13} \simeq 10^\circ$.) Thus, the uncertainty in θ_{13} is less dependent on the uncertainty in θ_{12} than the uncertainties in A_{n-d} and Δm^2 . We observe that the precise value of the partial derivatives depend on the point of evaluation, but that the values presented give a notion about their magnitudes. If we instead of Eq. (39) use a more optimistic estimate, then $\delta\theta_{13}$ reduces to about 8° . Unfortunately, this is still a quite large uncertainty and in order to reach an uncertainty of about 1° , we need measurements of A_{n-d} and Δm^2 with uncertainties that are about 100 times smaller than the uncertainties of today and a measurement of θ_{12} with an uncertainty that is about 10 times smaller than today.

5. Summary and conclusions

We have derived analytical expressions for the day P_S and night P_{SE} survival probabilities for solar neutrinos in the case of three neutrino flavors. The analytical result has been used to numerically study the qualitative effect of a non-zero θ_{13} mixing on the day-night asymmetry A_{n-d} at detectors. The regenerative term in the three flavor framework was found to be

$$\begin{aligned} P_{n-d} &= -c_{13}^6 D_{3\nu} \frac{KV_E}{4a^2} \sin^2(2\theta_{12}) \sin^2(aL) \\ &\simeq -c_{13}^6 D_{3\nu} \frac{2EV_E}{\Delta m^2} \sin^2(2\theta_{12}) \\ &\quad \times \sin^2\left(\frac{\Delta m^2}{4E}L\right), \end{aligned} \quad (40)$$

where $K = \Delta m^2/(2E)$ and the approximation is good for all parts of the LMA region. We have

also noted that we regain the two flavor expression for the regenerative term when $\theta_{13} \rightarrow 0$. An important observation is that the quantitative result depends linearly on the effective Earth electron density number used to calculate the regenerative term. We have argued that the value to be used is that of the Earth's crust.

In the study of the day-night asymmetry at detectors, it is apparent that the relative effect of a non-zero θ_{13} in the LMA region is increasing for increasing Δm^2 and decreasing θ_{12} and measured electron energy T . The dependence on θ_{12} is also larger for smaller T and larger Δm^2 . This result holds for both the elastic scattering and charged-current detection of neutrinos.

We have also shown that the effects of a non-zero θ_{13} on the isocontours of constant day-night asymmetry A_{n-d} at detectors are small compared to the current experimental uncertainty in A_{n-d} . However, should this uncertainty and the uncertainties in the fundamental parameters θ_{12} and Δm^2 become much smaller in the future, the day-night asymmetry could be used to determine θ_{13} as an alternative to future long baseline and reactor experiments.

Acknowledgments

We would like to thank Walter Winter for useful discussions and Thomas Schwetz for providing the data of the allowed θ_{12} - Δm^2 parameter space.

This work was supported by the Swedish Research Council (Vetenskapsrådet), Contract No. 621-2001-1611, 621-2002-3577 [T.O.], 621-2001-1978 [H.S.] and the Göran Gustafsson Foundation (Göran Gustafssons Stiftelse) [T.O.].

A. The case of two neutrino flavors

In the two flavor case, we use the parameterization

$$U = \begin{pmatrix} c & s \\ -s & c \end{pmatrix}, \quad (41)$$

where $s = \sin\theta$ and $c = \cos\theta$, for the leptonic mixing matrix. In this case, we can also write P_{SE} as a function of P_S and P_{2e} only such that

$$P_{n-d} = P_{SE} - P_S = \frac{1 - 2P_S}{\cos(2\theta)} (P_{2e} - \sin^2\theta). \quad (42)$$

For k_1 and k_2 , a general parameterization is

$$k_1 = \frac{1 + D_{2\nu}}{2}, \quad k_2 = \frac{1 - D_{2\nu}}{2}. \quad (43)$$

If we assume that all transitions among the matter eigenstates are incoherent and/or negligible in magnitude, then k_1 and k_2 are also given by

$$k_i = \int_0^{R_\odot} dr f(r) (\cos^2 \hat{\theta}(r) P_{1i}^s + \sin^2 \hat{\theta}(r) P_{2i}^s), \quad (44)$$

where $i \in \{1, 2\}$, P_{ki}^s is the probability of a neutrino in the mass eigenstate $|\nu_{M,k}\rangle$ at position r to exit the Sun in the state $|\nu_i\rangle$, $\hat{\theta}$ is the mixing angle in matter, and $f(r)$ is the normalized spatial distribution function of the production of neutrinos. Using this, we obtain $D_{2\nu}$ as

$$D_{2\nu} = \int_0^{R_\odot} dr f(r) \cos(2\hat{\theta}(r)) (1 - 2P_{\text{jump}}), \quad (45)$$

where $P_{\text{jump}} = P_{12}^s = P_{21}^s$. From this expression, it is easy to find that $|D_{2\nu}| \leq 1$, and thus, $0 \leq k_i \leq 1$, which is obviously a necessary condition. For the LMA solution of the solar neutrino problem, we obtain $P_{\text{jump}} < 10^{-1700}$ by using a linear approximation of the effective potential at the point of resonance. This is clearly negligible. The value of $\cos(2\hat{\theta})$ is calculated as

$$\cos(2\hat{\theta}) = \frac{K \cos(2\theta) - V_{CC}}{\sqrt{(K \cos(2\theta) - V_{CC})^2 + K^2 \sin^2(2\theta)}}, \quad (46)$$

where V_{CC} is the effective matter density potential. Now, the survival probability P_S takes the simple form

$$P_S = \frac{1 + D_{2\nu} \cos(2\theta)}{2}. \quad (47)$$

For the propagation inside the Earth, we make the approximation that the neutrinos traverse a sphere of constant electron number density. This approximation is motivated by the fact that for current detectors, most neutrinos do not pass through the Earth's core. As long as neutrinos do

not pass through the core, the only major non-adiabatic point of the neutrino evolution is the entry into the Earth's crust. As we will see, the regenerative term $P_{n-d} = P_{SE} - P_S$ will oscillate quickly with L and give an effective averaging. It follows that the exact nature of the adiabatic process inside the Earth does not matter as it only affects the frequency of the oscillations. Thus, we may use any adiabatic electron number density profile as long as we keep the electron number density at entry into the Earth's crust and at detection fixed to the correct values. In this case, the electron number density at entry into the crust and at detection are the same, namely the electron number density in the crust.

Keeping the electron number density constant, also the effective electron neutrino potential is kept constant at $V_E = \sqrt{2}G_F N_e$ where G_F is the Fermi coupling constant and N_e is the electron number density. Exponentiating the Hamiltonian, we obtain the time evolution operator and may calculate the probability P_{2e} . The result of this calculation is

$$P_{2e} = \sin^2 \theta + \frac{KV_E}{4a^2} \sin^2(2\theta) \sin^2(aL), \quad (48)$$

where

$$a = \frac{1}{2} \sqrt{K^2 - 2KV_E \cos(2\theta) + V_E^2}. \quad (49)$$

Using the above results, we calculate P_{n-d} and obtain the result

$$P_{n-d} = -D_{2\nu} \frac{KV_E}{4a^2} \sin^2(2\theta) \sin^2(aL). \quad (50)$$

For the allowed parameter space, the oscillation length in matter is given by $L_{\text{osc}} = 1/(2a) \simeq 1/K \sim 5 \cdot 10^4$ m, which is much shorter than the diameter of the Earth. Thus, we will have an effective averaging of the term $\sin^2(aL)$ in Eq. (50).

The expression for P_{n-d} contains many expected features. For example, when $V_E = 0$ then $P_{n-d} = 0$, the oscillation frequency is just the one that we expect, and $P_{n-d} = 0$ for $D_{2\nu} = 0$ reflecting the fact that this corresponds to $k_1 = k_2 = 1/2$. In Eq. (50), we observe that the sign of P_{n-d} depends on the sign of $D_{2\nu}$, which depends on the point of production. If we suppose

that $P_{\text{jump}} \ll 1$, then from Eq. (46) we find that $D_{2\nu}$ is negative if V_{CC} is larger than the resonance potential and positive if V_{CC} is smaller than the resonance potential. If the production occurs near the resonance, then $D_{2\nu}$ will be small, since $\hat{\theta} \simeq 45^\circ$ in this case. For the allowed parameter space, the region of production for ${}^8\text{B}$ neutrinos is such that V_{CC} is larger than the resonance potential, and thus, $D_{2\nu}$ will be negative. The same is true for $D_{3\nu}$.

REFERENCES

1. Super-Kamiokande Collaboration, Y. Fukuda et al., Phys. Rev. Lett. 81 (1998) 1562, [hep-ex/9807003](#); 82 (1999) 2644, [hep-ex/9812014](#); S. Fukuda et al., Phys. Rev. Lett. 86 (2001) 5651, [hep-ex/0103032](#); Phys. Lett. B539 (2002) 179, [hep-ex/0205075](#).
2. SNO Collaboration, Q.R. Ahmad et al., Phys. Rev. Lett. 87 (2001) 071301, [nucl-ex/0106015](#).
3. SNO Collaboration, Q.R. Ahmad et al., Phys. Rev. Lett. 89 (2002) 011301, [nucl-ex/0204008](#).
4. SNO Collaboration, Q.R. Ahmad et al., Phys. Rev. Lett. 89 (2002) 011302, [nucl-ex/0204009](#).
5. SNO Collaboration, S.N. Ahmed et al., [nucl-ex/0309004](#).
6. KamLAND Collaboration, K. Eguchi et al., Phys. Rev. Lett. 90 (2003) 021802, [hep-ex/0212021](#).
7. Super-Kamiokande Collaboration, M.B. Smy et al., [hep-ex/0309011](#).
8. L. Wolfenstein, Phys. Rev. D17 (1978) 2369; S.P. Mikheev and A.Y. Smirnov, Sov. Phys. Usp. 30 (1987) 759.
9. E.D. Carlson, Phys. Rev. D34 (1986) 1454; A.J. Baltz and J. Weneser, Phys. Rev. D35 (1987) 528; D50 (1994) 5971; E. Lisi and D. Montanino, Phys. Rev. D56 (1997) 1792, [hep-ph/9702343](#); J.N. Bahcall and P.I. Krastev, Phys. Rev. C56 (1997) 2839, [hep-ph/9706239](#); Q.Y. Liu, M. Maris and S.T. Petcov, Phys. Rev. D56 (1997) 5991, [hep-ph/9702361](#); M. Maris and S.T. Petcov, Phys. Rev. D56 (1997) 7444, [hep-ph/9705392](#); D58 (1998) 113008, [hep-ph/9803244](#); D62 (2000) 093006, [hep-ph/0003301](#); G.L. Fogli et al., Phys. Rev. D62 (2000) 113003, [hep-ph/0008012](#); C.W. Chiang and L. Wolfenstein, Phys. Rev. D63 (2001) 057303, [hep-ph/0010213](#).
10. A.H. Guth, L. Randall and M. Serna, JHEP 08 (1999) 018, [hep-ph/9903464](#).
11. A.S. Dighe, Q.Y. Liu and A.Y. Smirnov, (1999), [hep-ph/9903329](#).
12. P.C. de Holanda and A.Y. Smirnov, [hep-ph/0309299](#).
13. A. Bandyopadhyay et al., [hep-ph/0309174](#).
14. A.M. Dziewonski and D.L. Anderson, Phys. Earth Planet. Interiors 25 (1981) 297.
15. CHOOZ Collaboration, M. Apollonio et al., Phys. Lett. B466 (1999) 415, [hep-ex/9907037](#); Eur. Phys. J. C27 (2003) 331, [hep-ex/0301017](#).
16. Particle Data Group, K. Hagiwara et al., Phys. Rev. D66 (2002) 010001.
17. J.N. Bahcall, M.H. Pinsonneault and S. Basu, Astrophys. J. 555 (2001) 990, [astro-ph/0010346](#).
18. M. Maltoni et al., [hep-ph/0309130](#).
19. <http://www.sns.ias.edu/~jnb/>, Homepage of J.N. Bahcall.
20. P. Huber, M. Lindner and W. Winter, Nucl. Phys. B645 (2002) 3, [hep-ph/0204352](#).
21. M. Apollonio et al., [hep-ph/0210192](#); Muon Collider/Neutrino Factory Collaboration, M.M. Alsharoa et al., Phys. Rev. ST Accel. Beams 6 (2003) 081001, [hep-ex/0207031](#).
22. P. Huber et al., Nucl. Phys. B665 (2003) 487, [hep-ph/0303232](#).
23. Y. Itow et al., [hep-ex/0106019](#); D. Ayres et al., [hep-ex/0210005](#).
24. A.S. Dighe, M.T. Keil and G.G. Raffelt, JCAP 0306 (2003) 006, [hep-ph/0304150](#).
25. S. Ando et al., Phys. Lett. B555 (2003) 49, [nucl-th/0206001](#).
26. <http://www.sno.phy.queensu.ca/sno/>, SNO HOWTO kit.
27. A. Bandyopadhyay, S. Choubey and S. Goswami, Phys. Rev. D 67 (2003) 113011, [hep-ph/0302243](#).